

THE GROUNDSTATES AND PHASES OF THE TWO-DIMENSIONAL FULLY FRUSTRATED XY MODEL

PETTER MINNHAGEN and SEBASTIAN BERNHARDSSON

*Department of Physics, Umeå University,
Umeå, 90187, Sweden
minnhagen@tp.umu.se*

BEOM JUN KIM

*BK21 Physics Research Division and Institute of Basic Science,
Sungkyunkwan University, Suwon, 440-746, Korea
beomjun@skku.edu*

Received 24 July 2009

The 2D Fully Frustrated XY (FFXY) class of models is shown to contain a new groundstate in addition to the checkerboard groundstate of the standard 2D XY model. The spin configuration of this additional groundstate is obtained and its connection to a broken Z_2 -symmetry explained. This means that the class of 2D FFX models belongs within a $U(1) \otimes Z_2 \otimes Z_2$ -symmetry phase-transition representation. The phase diagram is reviewed and the central charges of the four multicritical points described. The implications for the standard 2D FFX model are discussed and elucidated, in particular with respect to the long standing controversy concerning the phase transitions of the standard 2D FFX model.

1. Introduction

The two-dimensional (2D) XY-model is one of the prototypes in the area of phase transitions. It can be viewed as an extension of the Ising model in which the planar spins of unit lengths are augmented by directions described by angles with respect to some fixed direction in space. The notable feature is that it undergoes a Kosterlitz-Thouless (KT) transition from a low-temperature ordered phase to a high-temperature disordered phase.^{1,2,3,4} The KT-transition is associated with the angular $U(1)$ -symmetry of the Hamiltonian for the XY-model. As a result of this continuous angular symmetry the spin correlation can in two dimensions only be “quasi” ordered in the low-temperature phase: the spin correlation function has a power-law decay with distance in the low-temperature phase.⁵ This also means that the KT-transition is not associated with a local order parameter. Instead the transition is associated with the helicity modulus which is a global property of the system.⁴ From a symmetry point of view this means that the $U(1)$ -symmetry of the Hamiltonian is only “quasi” broken in the low-temperature phase.

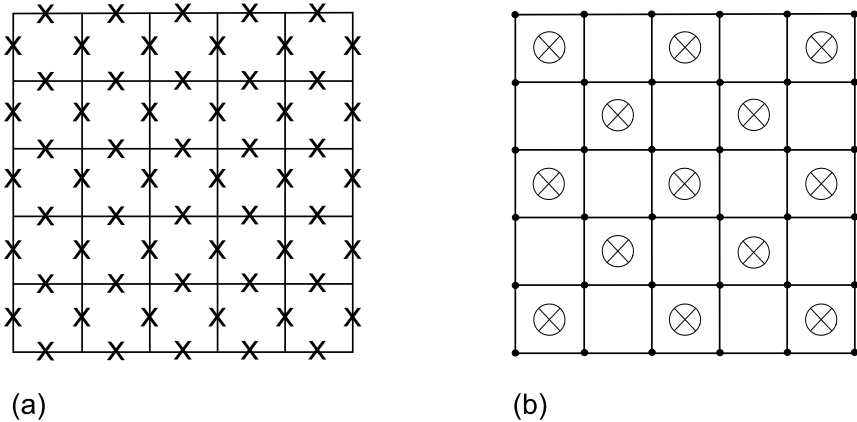


Fig. 1. (a) Schematic diagram of two-dimensional Josephson junction array and (b) the checkerboard type vortex configuration of the groundstate for the 2D FFXY model corresponding to (a). In (a), crosses denote Josephson junctions and superconducting islands are at each node of squares. Vortices are marked as crosses at every second plaquettes in (b).

Examples of physical systems which can be described by the XY-model are magnetic spin systems in which one component of the spins are suppressed and a superconductor. In case of the superconductor the spin angle corresponds to the phase of the local superconducting order parameter. In particular a two-dimensional (2D) Josephson junction array can be very directly mapped to the 2D XY-model (see Fig. 1a).⁶

The model of particular interest here is the 2D fully frustrated XY (FFXY)-model which corresponds to a Josephson array in a perpendicular magnetic field with the strength of the magnetic field corresponding to a magnetic flux quanta for every second plaquette of the array (see Fig. 1b).⁷

The groundstate for the 2D FFXY model is the checkerboard pattern shown in Fig. 1b. There are two identical possibilities since translating the checkerboard pattern by one square leaves the Hamiltonian invariant. This reflects that the Hamiltonian of the 2D FFXY model in addition to the $\mathcal{U}(1)$ -symmetry also contains a Z_2 -symmetry associated with the two possible groundstate patterns. This Z_2 -symmetry is broken for low enough temperatures and is described by a local order parameter. Thus the Hamiltonian of the 2D FFXY model has two spin symmetries that can be broken (or “quasi” broken), i.e. a $\mathcal{U}(1)$ and a Z_2 : it can be assigned the combined symmetry $\mathcal{U}(1) \otimes Z_2$.

The character and the order of the phase transitions for the 2D FFXY-model have been the subject of a long controversy.^{8,9,10,11,12,13,14,15} This is because the two transitions appear to be extraordinary close. As a consequence a combined single $\mathcal{U}(1) \otimes Z_2$ with critical properties described by a single critical point has also been judged to be consistent with earlier simulations.^{8,9,12,16,14} However, the emerging consensus is two separate transitions: as the temperature is increased first a KT-

transition associated with the angular $\mathcal{U}(1)$ -symmetry and then at a slightly higher temperature a Z_2 -symmetry transition.⁸

In the present paper, we study an extended class of 2D FFXY models. The Hamiltonians for this class have the same spin symmetries as the 2D FFXY model: the spin interaction potential is modified in such a way as to keep all the spin symmetries. For example the much studied Villain model is obtained from the 2D FFXY by such a modification and belongs to the extended class.¹⁷ One purpose of this type of modifications is to obtain a better understanding of the original model. In the present work we study the Two-Dimensional Generalized Fully Frustrated XY (2D GFFXY) model which belongs to the 2D FFXY-class and parametrizes a systematic change of the interaction potential.¹⁸ The 2D GFFXY-model turns out to have a complex phase diagram.^{18,19} In the present paper we relate this complexity to the occurrence of a new groundstate for which the checkerboard Z_2 -symmetry is restored. The spin configuration for this groundstate is obtained. In particular we discuss the implications of this new groundstate for the understanding of the original 2D FFXY-model.

In section 2 we define the 2D FFXY-model and in section 3 we describe the structure of the new ground state. In section 4 we describe the order parameter and the broken symmetry associated with the transition into this new groundstate. We review the phase diagram in section 5 as well as the conformal charges associated with the various multicritical points. Finally, in section 6 we discuss the original 2D FFXY model in view of the results for the 2D GFFXY model.

2. Generalized 2D XY Model

The Hamiltonian which defines the 2D fully frustrated XY-class models on an $L \times L$ square lattice is given by

$$H = \sum_{\langle ij \rangle} U(\phi_{ij} \equiv \theta_i - \theta_j - A_{ij}), \quad (1)$$

with $\phi_{ij} \in [-\pi, \pi]$, where the sum is over nearest neighbor pairs. The phase angle θ_i for the i th site at the lattice point (x_i, y_i) satisfies the periodicity $\theta_{i+L\hat{x}} = \theta_{i+L\hat{y}} = \theta_i$. The magnetic bond angle A_{ij} is defined as the line integral along the link from i to j , i.e., $A_{ij} \equiv (2\pi/\Phi_0) \int_i^j \mathbf{A} \cdot d\mathbf{l}$ with the magnetic vector potential \mathbf{A} for the uniform magnetic field $\mathbf{B} = B_0 \hat{z}$ in the z direction. With the Landau gauge taken, $A_{ij} = 2\pi f x_i$ for the vertical link and $A_{ij} = 0$ for the horizontal one, where the frustration parameter f measures the average number of flux quanta per plaquette, i.e., $f = B_0/\Phi_0$ with the flux quantum Φ_0 (the lattice constant has been set to $a \equiv 1$). The fully frustrated case corresponds to $f = 1/2$ and a half flux quantum per plaquette on the average. The Boltzmann factor, which determines the thermodynamic properties, is given by $\exp(-H/T)$ where T is the temperature. The interaction potential $U(\phi) = U(\phi \pm 2\pi)$ is periodic in 2π and is given by^{20,21}

$$U(\phi) = \frac{2}{p^2} \left[1 - \cos^{2p^2} \left(\frac{\phi}{2} \right) \right], \quad (2)$$

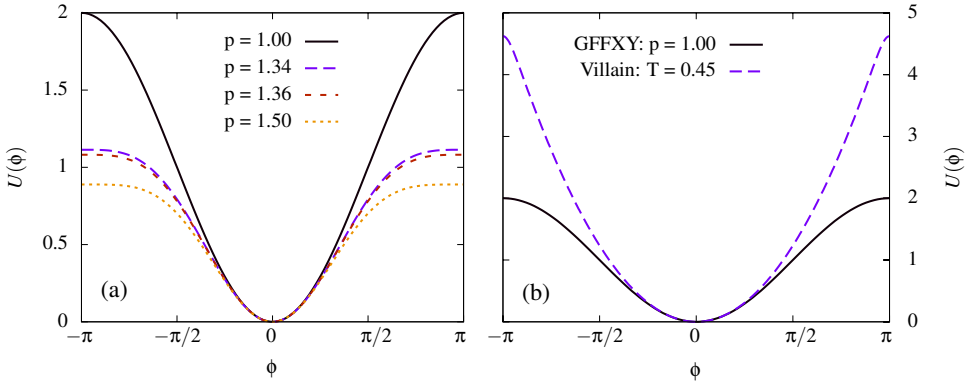


Fig. 2. Interaction potentials $U(\phi)$ in Eq. (2) at various values of p are compared in (a). The standard XY model corresponding to $p = 1$ is also compared with the Villain interaction potential in (b). All interactions have the same symmetry and have the identical quadratic form at small ϕ .

where $p = 1$ corresponds to the standard FFXY since $2[1 - \cos^2(\phi/2)] = 1 - \cos(\phi)$. The interaction potential $U(\phi)$ is shown in Fig. 2a for a sequence of p -values. The interaction within the 2D XY-class is characterized by being periodic in 2π , quadratic to the lowest order in ϕ so that $U(\phi) \sim \phi^2$, and monotonically increasing from zero in the interval $[0, \pi]$. The interaction potential defines the class: the various members of this class are distinguished by the explicit form of $U(\phi)$. In Fig. 2b the interaction potential for the standard XY model $U(\phi) = 1 - \cos(\phi)$ is compared to the one for the Villain model at the KT-transition ($T = 0.45$) $U(\phi) = -T \ln\{\sum_{n=-\infty}^{n=\infty} \exp(-(\phi - 2\pi n)^2/2T)\}$.^{17,8} The 2D FFXY model with the Villain interaction has the same phase transition scenario as the the usual 2D FFXY model i.e. a $U(1)$ KT-transition followed by a Z_2 transition (still extremely close together but a little less close than for the standard 2D FFXY model).⁸ Is this true for all models within the XY class? The answer is no.¹⁸ The reason is connected to the appearance of a new groundstate.

3. Groundstate

Let us first consider the groundstate for the standard 2D FFXY model on a square lattice: The spin configuration corresponding to the groundstate checkerboard is given in Fig. 3a.²² A square with (without) a flux quanta is denoted by + (-). The arrows give the spin directions and the thick (thin) links are the links with (without) magnetic bond angles π (0) modulo 2π . In this configuration all the links contribute the same energy $U(\frac{\pi}{4})$ to the groundstate. Thus the energy for the four links constituting an elementary square is in this configuration $4U(\frac{\pi}{4})$. The broken symmetry of the free energy is for $T = 0$ directly related to the fact that in order to change + to - squares in Fig. 3a by continuously turning the spin directions from the one groundstate to the other, an increase of the energy is required by a finite

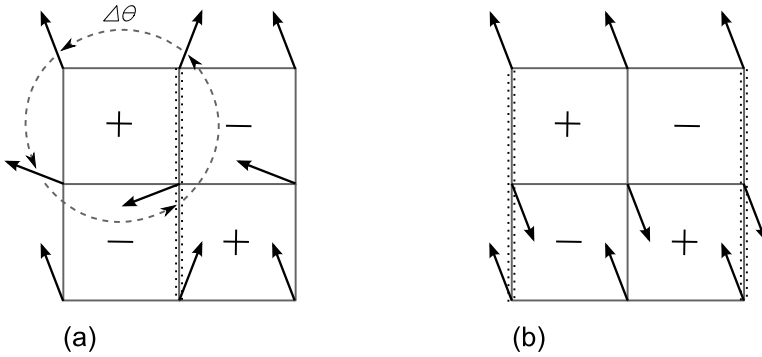


Fig. 3. Two groups of distinct groundstates of the 2D GFFXY model. (a) When p is smaller than p_c (≈ 1.3479), the gauge-invariant phase difference $\phi = \pi/4$ for all edges of a plaquette. (b) When $p > p_c$, one edge has $\phi = \pi$ while all other three have $\phi = 0$. The wiggled vertical lines denote the magnetic bond angles $A_{ij} = \pi$, arrows indicate phase values, and \pm represents vortex charges.

amount of a number of links. This number of links goes to infinity with the size of the system: the two groundstates are separated by an infinite energy barrier.

The crucial point in the present context is that the groundstate shown in Fig. 3a does not remain as the groundstate for all values p . As p is increased the maximum link energy $U(\pi)$ decreases and at a particular value $p_c > 1$ the groundstate switches to the spin configuration shown in Fig. 3b. The energy for the links around a square is for this configuration given by $U(\pi) + 3U(0)$. The critical value p_c is hence given by the condition $U(\pi) + 3U(0) = 4U(\frac{\pi}{4})$ leading to the determination

$$p_c = \sqrt{\frac{\ln(3/4)}{2\ln(\cos(\pi/8))}} = 1.3479. \quad (3)$$

The groundstate for $p > p_c$ shown in Fig. 3b has the property that an infinitesimal change of the middle spin is enough to flip between the two checkerboard patterns (switching between $+$ and $-$ in Fig. 3b). Thus there is no barrier between these two checkerboard patterns for $p > p_c$. This means that the broken symmetry of the free energy associated with the two possible checkerboard patterns states is restored. However, there is a new infinite barrier between the two degenerate groundstates on opposite sides of p_c : continuously turning the spins to change from the spin-configuration in Fig. 3a to the spin-configuration in Fig. 3b requires an infinite energy.

4. Broken Symmetries

We are here interested in the phase transition properties of the 2D GFFXY model. To this end we need to identify the relevant order parameters associated with the broken symmetries of the free energy. The broken checkerboard pattern is usually referred to as the Z_2 chirality symmetry. The corresponding order parameter is the

staggered magnetization m defined as ⁷

$$m = \left\langle \left| \frac{1}{L^2} \sum_{l=1}^{L^2} (-1)^{x_l+y_l} s_l \right| \right\rangle, \quad (4)$$

where $\langle \dots \rangle$ is the ensemble average and the vorticity for the l th elementary plaquette at (x_l, y_l) is computed from $s_l \equiv (1/\pi) \sum_{\langle ij \rangle \in l} \phi_{ij} = \pm 1$ with the sum taken in the anti-clockwise around the given plaquette. The broken symmetry is reflected in the following way: for any finite system the quantity $\frac{1}{L^2} \sum_{l=1}^{L^2} (-1)^{x_l+y_l} s_l$ can with finite probability acquire any value in the range $[-1, 1]$ allowed by the Hamiltonian. However, in the thermodynamic limit $L = \infty$ only values in the either the range $[-1, 0]$ or the range $[0, 1]$ can be acquired. In the latter case $m \neq 0$ whereas in the former case when the symmetry is unbroken $m = 0$.

The broken symmetry between the two groundstates shown in Fig. 3a and b is associated with an additional Z_2 -symmetry of the free energy. The quantity related to this symmetry breaking is the kink density n_k defined as

$$n_k = \left\langle \frac{4}{L^2} \sum_{t=1}^{\frac{L^2}{4}} |s_t| \right\rangle, \quad (5)$$

where the square lattice has been divided into $L^2/4$ squares numerated by t where each consists of four elementary plaquettes. Here s_t is the sum of the phase difference around a four-plaquette $s_t \equiv (1/\pi) \sum_{\langle ij \rangle \in t} \phi_{ij}$ which means that $|s_t|$ can be 0, 1 or 2. The kink concept is illustrated in Fig. 4: start from a checkerboard pattern. The thick dotted line is a boundary between the two possible checkerboard patterns. The 90 degree turn of this line is associated with a four-plaquette with $s_t = 1$ which is denoted as thick solid line surrounding four plaquettes in Fig. 4. The kink density n_k plays the same role as the density in a usual liquid-gas transition: the order parameter is the density-difference, Δn_k , between a low- and high-density phase. Just as for a liquid-gas transition it is associated with a Z_2 broken symmetry.

As mentioned above $\mathcal{U}(1)$ -symmetry is at most “quasi” broken and can hence not be associated with a local order parameter. Instead it can be monitored by the increase of the free energy caused by a uniform twist δ of the spin angles across the system. Expanding the free energy $F(\delta)$ for small values of δ to lowest orders gives

$$F(\delta) = Y \frac{\delta^2}{2} + Y_4 \frac{\delta^4}{4!}. \quad (6)$$

Here, Y is the helicity modulus. It is finite in the low-temperature phase and zero in the high-temperature phase.⁴ Y_4 is the fourth order modulus and can be used to verify that the helicity modulus Y makes a discontinuous jump to zero at the transition.²³ This discontinuous jump is a key characteristics of the KT-transition.^{24,25}

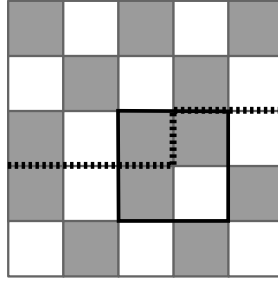


Fig. 4. Two checkerboard states with the boundary between them (denoted as thick dotted line). A kink exists where the boundary makes a 90-degree turn, and the kink density n_k is measured by Eq. (5). For the four plaquettes surrounded by thick full line, $|s_t| = 1$ whereas all other four plaquettes have even number of vortices and thus $|s_t| = 0$.

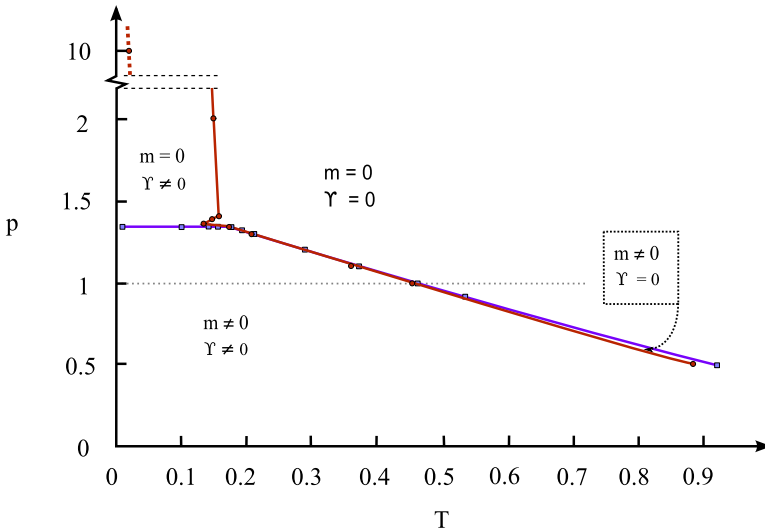


Fig. 5. Phase diagram of the 2D GFFXY model in the (p, T) plane. The staggered magnetization m and the helicity modulus Y give us all four combinations, all of which are realized in the phase diagram. The horizontal dotted line at $p = 1$ corresponds to the standard FFXY model which has two distinct, extremely close transitions.

5. Phase Transitions and Phase Diagram

The phase diagram of the 2D GFFXY model was obtained in Ref. 18 by Monte Carlo Simulations and is shown in Fig. 5. It contains 4 sectors characterized by the four possible combinations of the two order parameters m and Y : $(m, Y) = (0, 0)$, $(0, \neq 0)$, $(\neq 0, 0)$ and $(\neq 0, \neq 0)$. The standard 2D FFXY model corresponds to the dotted line $p = 1$ and as the temperature increases from $T = 0$ it departs from the checkerboard groundstate characterized by $(m, Y) = (\neq 0, \neq 0)$, makes a KT

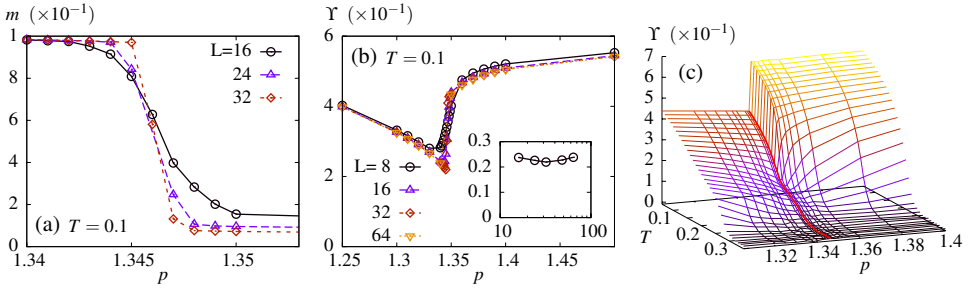


Fig. 6. (a) Z_2 -chirality symmetry breaking transition is detected by the staggered magnetization m at $T = 0.1$ as p is varied. The Z_2 transition in (a) is not accompanied by the $U(1)$ transition as shown in (b) for the helicity modulus Y which remains non-zero in either side of the transition. In inset of (b), Y is shown as a function of L , confirming $Y \neq 0$ in thermodynamic limit. (c) Y in the (p, T) plane. The cusp-like structure at low T disappears as T is increased.

transition at $T \approx 0.446$ into $(m, Y) = (\neq 0, 0)$ followed by Z_2 -transition at $T \approx 0.454$ into the high-temperature phase $(m, Y) = (0, 0)$ for which all broken symmetries are restored. The notable feature is the extreme narrowness of the $(m, Y) = (\neq 0, 0)$ -phase. As mentioned in the introduction this narrowness caused a long controversy as to whether in fact there is just one joint transition and no intermediate phase $(m, Y) = (\neq 0, 0)$.

The new groundstate is associated with phase $(m, Y) = (0, \neq 0)$ appearing for p slightly larger than 1 (see Fig. 6). As is clear from the structure of the groundstate the staggered magnetization m is zero because there is no infinite energy barrier between the two checkerboard patterns in this phase: there is no broken Z_2 -symmetry associated with the checkerboard pattern in this phase. Figure 6a illustrates how $|m|$ vanishes with increasing L as the phase line from the $(m, Y) = (\neq 0, \neq 0)$ to the $(m, Y) = (0, \neq 0)$ is passed at $T = 0.1$.¹⁸ What is less obvious from the groundstate is that Y remains non-zero as the same phase line is passed. The fact that Y remains non-zero is shown in Fig. 6 b: the helicity modulus Y remains non-zero on both sides of the phase line. It has a small dip right on the phase line but, as the inset shows, remains non-zero also on the phase line. Figure 6c shows in which regions Y is finite.

As is apparent from Fig. 5 and 6, $(m, Y) = (0, 0)$, $(0, \neq 0)$, $(\neq 0, 0)$ and $(\neq 0, \neq 0)$ classifies all the possible phases of the 2D GFFXY model. However, the classification of the the phase transitions and the multicritical points are more complicated. As illustrated in Fig. 7, the phase diagram contains four multicritical points A, B, C, and D.¹⁹ The reason for this complicated phase transition scenario is the additional broken Z_2 -symmetry associated with the kink density n_k . Let us start with the phase line from $(p, T) = (p_c, 0)$ to A. Figure 8a illustrates that this phase transition line is associated with a broken symmetry: The double hump in the distribution of n_k . This distribution $P(n_k)$ is related to the free energy F by $P(n_k) \sim \exp(-F(n_k)/T)$ and the two humps are separated by the free energy barrier $\Delta F \sim -\ln[P(n_k)]$ which

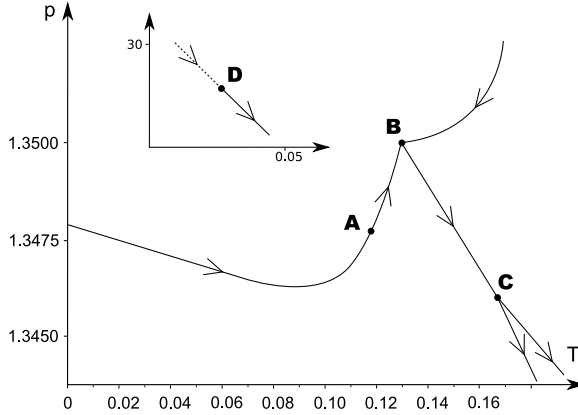


Fig. 7. Expansion of the phase diagram near $p_c \approx 1.3479$ (compare with Fig. 5). There are in total four multicritical points (see text).

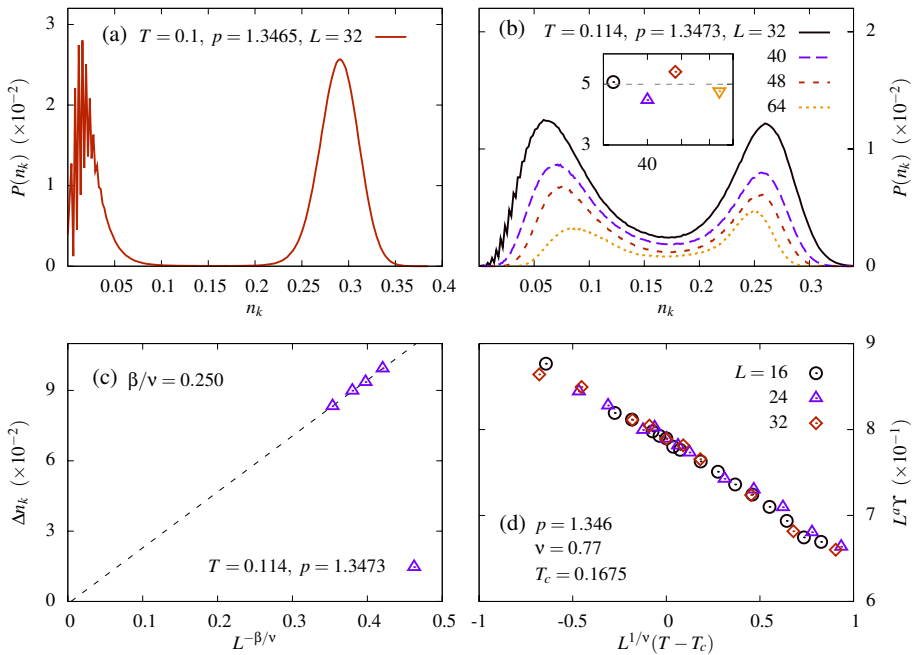


Fig. 8. (a) The kink density distribution function $P(n_k)$ at $T = 0.1$ and $p = 1.3465$ (on the phase transition line starting at $T = 0$ in Fig. 7). The difference between the two peak Δn_k exhibits a discontinuous transition. (b) At the multicritical point A in Fig. 7, $P(n_k)$ shows continuous transition which is well described by the critical exponent $\beta/\nu = 0.25$ as displayed in (c). (d) At the multicritical point C in Fig. 7, the helicity modulus Y does not have a finite jump but exhibits a continuous transition with $\nu = 0.77$.

becomes infinite whenever $P(n_k) \rightarrow 0$ for large L . This is the case for the minimum in Fig. 8a. Consequently, the free energy symmetry is broken, since the possible values are separated by an infinite barrier in the thermodynamic limit. However this double hump structure ceases to exist beyond the critical point A. On the left-hand side of A the distance between the two humps remains finite for $L \rightarrow \infty$ which signals a first order discontinuous transition. To the right of A there is only one hump and $P(n_k)$ remains finite for all values of n_k for $L \rightarrow \infty$. Precisely at the point A $P(n_k) \rightarrow 0$ and the distance between the two humps vanishes for $L \rightarrow \infty$ (see Fig. 8b). The order parameter is the distance between the peak position of the two humps Δn_k . It vanishes as $\Delta n_k \sim L^{-\beta/\nu}$ and this ratio between the critical indices β and ν was in ¹⁹ found to be consistent with $\beta/\nu = 0.25$ (see Fig. 8c). Thus the symmetry breaking associated with the kink density n_k is from $(p, T) = (p_c, 0)$ to A connected to a first order transition which ends at the second order critical point A. This is reminiscent of a liquid-gas transition. However, also the staggered magnetization m makes a transition across the line from $(p, T) = (p_c, 0)$ to A because the broken Z_2 checkerboard symmetry gets restored. This transition is also contained in the first order transition which ends at A. The difference is that this checkerboard transition does not cease but continues to the multicritical point B. On the phase transition line between the points A and B, m vanishes as $|m| \sim L^{-\beta/\nu}$ with $\beta/\nu = 0.125$.¹⁹ This is the same β/ν -value as for the usual Z_2 -transition of the 2D Ising model. At the critical point B the checkerboard transition meets the KT-transition coming from above and both transitions continue as a single joint transition to the multicritical point C. Along this phase line and also on the critical points B and C, m vanishes as $|m| \sim L^{-\beta/\nu}$ with $\beta/\nu = 0.375$.¹⁹ At the multicritical point C the joint transition splits into two separate transitions with the KT transition to the left at lower T and the checkerboard transition to the right at higher. Finally the critical point D, at much higher p and lower T is the starting point for the KT-transition line and the end point of a first order joint n_k -KT transition, quite similar to the end point A of the first order joint n_k - m transition.¹⁹

The multicritical point C is of special interest in the present context because its closeness to and possible influence on the phase transitions of the standard 2D FFXV-model. At the critical point C (as well as along the phase line between B to C) the helicity modulus Y does not undergo a KT transition with a discontinuous jump, but goes to zero as $Y \sim L^{-a}$ where $a \approx 0.63$ precisely at C. From the finite-size scaling $Y = L^{-a}g((T - T_{cC})L^{1/\nu})$ also the critical index $\nu \approx 0.77$ is found (see Fig. 8d).¹⁹

6. Central Charge

Conformal field theory in two dimensions establishes a link between the broken symmetries and the characteristics of the phase transitions.²⁶ This connection can be expressed as a direct relation between the central charge c and the ratio of critical indices β/ν given by $\beta/\nu = c/4$.²⁶ The point is that the central charge c is coupled

to the broken symmetries: a single Z_2 -transition corresponds to $c = 1/2$ and a single $\mathcal{U}(1)$ to $c = 1$; a merged $Z_2 \otimes Z_2$ -transition to $c = 1$; a merged $\mathcal{U}(1) \otimes Z_2$ to $c = 3/2$, a merged $\mathcal{U}(1) \otimes Z_2 \otimes Z_2$ -transition to $c = 2$. This exhausts all the possibilities for the 2D GFFXY model. Applying this to the phase diagram in Fig. 7 and the values for β/ν obtained from MC simulations, we reach at the following conclusions: The multicritical point A displays a combined $Z_2 \otimes Z_2$ -transition involving the two broken symmetries related to the checkerboard pattern and the kink density. The multicritical points B and C is associated with a combined $\mathcal{U}(1) \otimes Z_2$ -transition ($c = 3/2$ and $\beta/\nu = 3/8$) involving the KT-transition and the checkerboard transition. This combined transition also describes the critical line between B and C. Finally the critical point D is a combined $\mathcal{U}(1) \otimes Z_2$ -transition involving the KT-transition and the kink-density transition.

7. Implications for Standard 2D FFXY Model

The usual 2D FFXY model corresponds to the $p = 1$ -line in Fig. 5. The critical point C for the 2D FFXY class is the closest multicritical point to the actual phase transitions of the usual 2D FFXY model (compare Fig. 7). The critical point C is characterized by the critical index $\nu \approx 0.77$ and the central charge $c = 1.5$. A single Z_2 transition is characterized by $\nu = 1$ and $c = 0.5$. All the earlier papers, in which it was concluded that the 2D FFXY model has only one joint transition, the apparent value of ν was in the interval $0.77 < \nu < 1$ (see table 1 in Ref. [8]). In particular in Ref. [12] the values of ν and c were independently determined and given by $\nu = 0.80(4)$ and $c = 1.61(3)$. Thus the apparent multicritical point for the usual FFXY model appeared to have critical properties inconsistent with a single Z_2 -transition and with critical ν -values in between a single Z_2 -transition and the real $\mathcal{U}(1) \otimes Z_2$ multicritical point C for the 2D FFXY class. Furthermore, the closeness of the ν -values and c -values, $\nu \approx 0.77$ and $c = 1.5$ for C, respectively, $\nu = 0.80(4)$ and $c = 1.61(3)$ determined for the usual FFXY model in Ref. 12, suggests that the apparent multicritical point found for the 2D FFXY model is an artifact of the closeness to the real critical point C for the 2D FFXY class.

The present consensus is that the 2D FFXY model undergoes two separate transition, a KT transition at T_{KT} followed by a Z_2 -transition at T_{Z_2} with $T_{KT} < T_{Z_2}$.⁸ In particular Korshunov in Ref. [15] has given a general argument which purportedly states that $T_{KT} < T_{Z_2}$ should be true not only for the 2D FFXY model, but also for the 2D FFXY class provided that the interaction is such that its groundstate is the broken symmetry checkerboard state. This is in contradiction with the existence of the multicritical point C which does correspond to such an interaction potential. We suggest that the reason for this fallacy of the argument is connected to the closeness to the $(m, Y)=(0, \neq 0)$ -phase.

The most striking feature of the phase transition for 2D FFXY model is the closeness between T_{KT} and T_{Z_2} . The phase diagram in Fig. 7 gives a scenario for which this feature becomes less surprising: The point is that the checkerboard tran-

sition and the KT-transition merge and cross as a function of p for the 2D GFFXY model. It then becomes more natural that for some values of p the transitions can be extremely close. The value $p = 1$, which corresponds to the usual FFFXY model happens to be such a value.

Acknowledgments

P.M. and S.B. acknowledge support from the Swedish Research Council grant 621-2002-4135. B.J.K. acknowledges the support by the KRF with grant no. KRF-2005-005-J11903.

References

1. V.L. Berezinskii, *Zh.Eksp. Teor. Fiz.* **59**, 907 (1970).
2. J.M. Kosterlitz and D.J. Thouless, *J. Phys. C* **7**, 1046 (1973).
3. J.M. Kosterlitz and D.J. Thouless, *J. Phys. C: Solid State Phys.* **18**, 2437 (1985).
4. P. Minnhagen, *Rev. Mod Phys* **59**, 1001 (1987).
5. N.D. Mermin and H. Wagner, *Phys. Rev. Lett.* **17**, 1133 (1966).
6. P. Martinoli and Ch. Leemann, *J. Low Temp. Phys.* **118**, 699 (2000).
7. S. Teitel and C. Jayapakrash, *Phys. Rev. B* **27**, 598 (1983).
8. M. Hasenbusch, A. Peissetto and E. Vicari *J.Stat.Mech. Theor. Exp.*, P12002 (2005).
9. E.Granato, J.M. Kosterlitz, J. Lee, and M.P. Nightingale, *Phys. Rev. Lett* **66**, 1090 (1991).
10. J. Lee, J.M. Kosterlitz and E. Granato, *Phys. Rev. B* **43**, 11531 (1991).
11. J. Lee, E. Granato and J.M. Kosterlitz, *Phys. Rev.B* **44**, 4819 (1991).
12. E. Granato and M.P. Nightingale, *Phys.Rev.B* **48**, 7438 (1993).
13. P. Olsson, *Phys. Rev. Lett* **75**, 2758 (1995).
14. E.H. Boubcher and H.T. Diep, *Phys. Rev. B* **58**, 5163 (1998).
15. S.E. Korshunov, *Phys. Rev. Lett* **88**, 167007 (2002).
16. M.P. Nightingale, E. Granato and J.M. Kosterlitz, *Phys.Rev.B* **52**, 7402 (1995).
17. J. Villain, *J. Phys. C* **10**, 1717 (1977).
18. P. Minnhagen, B.J. Kim, S. Bernhardsson and G. Cristofano, *Phys. Rev. B* **76**, 224403 (2007).
19. P. Minnhagen, B.J. Kim, S. Bernhardsson and G. Cristofano (preprint).
20. E. Domani, M. Schick and R. Swendsen, *Phys. Rev. Lett.* **52**, 1535 (1984).
21. A. Jonsson and P. Minnhagen, *Phys. Rev. Lett* **73**, 3576 (1994).
22. T. Halsey, *J. Phys. C* **18**, 2437 (1985).
23. P. Minnhagen and B.J. Kim, *Phys. Rev. B* **67**, 172509 (2003).
24. D. Nelson and J. M. Kosterlitz, *Phys. Rev. Lett.* **39**, 1201 (1977).
25. P. Minnhagen and G.G. Warren, *Phys. Rev. B* **24**, 6758 (1981).
26. P. Di Francesco, P. Mathieu and D. Senechal, *Conformal Field Theories* (Springer-Verlag, New York, 1997).